Retrieval of Cirrus Cloud Properties From the Atmospheric Infrared Sounder: The k-Coefficient Approach Using Cloud-Cleared Radiances as Input

Steve S. C. Ou, Brian Kahn, Kuo-Nan Liou, Yoshihide Takano, Mathias M. Schreier, and Qing Yue

***Abstract*—We have developed a k-coefficient retrieval approach for Atmospheric Infrared Sounder (AIRS) observations, using AIRS cloud-cleared radiances (ACCRs) as input. This new approach takes advantage of the available ACCR, reduces computational expense, offers an efficient and accurate cirrus cloud retrieval alternative for hyperspectral infrared (IR) observations, and is potentially applicable to the compilation of a long-term cirrus cloud climatology from hyperspectral IR observations. The retrieval combines a lookup-table method coupled to a residual minimization scheme using observed cloudy and cloud-cleared AIRS radiances as input. Six AIRS channels between 766 and 832 cm^{-1} with minimal water vapor absorption/emission have been selected, and their spectral radiances have been demonstrated to be sensitive to both cirrus cloud optical depth (τ_c) and ice crystal effective particle size (D_e). The capability of the k-coefficient approach is demonstrated by comparison with a more accurate retrieval program, which combines the delta-four stream (D4S) approximation with the currently operational Stand-alone AIRS Radiative Transfer Algorithm (SARTA). The distribution patterns and the range of retrieved cloud parameters from the k-coefficient approach are nearly identical to those from SARTA+D4S retrievals, with minor differences traced to uncertainties in parameterized cloudy radiances in the k-coefficient approach and in the ACCR. The k-coefficient approach has also been applied to four AIRS granules over North Central China, Mongolia, and Siberia containing a significant presence of cirrus clouds, and its results are quantitatively compared to simultaneous Moderate Resolution Imaging Spectroradiometer/Aqua cirrus cloud retrievals. Finally, AIRS retrieved τ_c and D_e are consistent with the Cloud-Aerosol Lidar and Infrared Pathfinder Satellite Observations (CALIPSO) and CloudSat derived values for semi-transparent cirrus clouds, with more significant differences in thicker cirrus and multilayer clouds.**

***Index Terms*—Atmospheric Infrared Sounder (AIRS), cirrus clouds, cloud-cleared radiances, ice crystal mean effective diameter, k-coefficient approach, Moderate Resolution Imaging Spectroradiometer (MODIS), optical depth, satellite remote sensing, Stand-alone AIRS Radiative Transfer Algorithm (SARTA), δ-four stream (D4S) method.**

I. Introduction

CIRRUS clouds are important regulators of the global radiation budget and climate. Based on satellite and ground-based observations, cirrus clouds cover 20%–30% of the Earth and up to 70% of the tropics at any given time. Since the atmospheric and surface radiative budget in cirrus cloudy conditions depends on cirrus cloud optical and microphysical parameters, it is necessary to determine the long-term statistics of these cirrus cloud parameters for input into detailed broadband radiative transfer models (RTMs) for computing cirrus cloud radiative forcings.

For mapping cirrus cloud fields, various satellite and airborne remote sensing approaches, including both solar and thermal infrared (IR) window two-channel correlation methods [1]–[3] and the 1.38-μm reflectance method [4], have been developed to retrieve optical and microphysical properties of cirrus clouds. Operational programs for global satellite remote sensing of these parameters using the Moderate Resolution Imaging Spectroradiometer (MODIS) data [5]–[7] and the split-window approach [8] for estimating cloud-top temperature and 11-μm cloud emissivity using the Advanced Very High Resolution Radiometer (AVHRR) data have been developed. The split-window approach generates the effective extinction coefficient ratio based on the single-scattering theory, using the MODIS bulk single-scattering property models [9], and it has been recently applied to produce a 30-year cloud climatology of the AVHRR Pathfinder Atmospheres Extended (PATMOS-x) data set and to the processing system of Clouds from AVHRR Extended. In addition, the Visible/Infrared Imager Radiometer Suite instrument on board the National Polar-Orbiting Operational Environmental Satellite System [10] Preparatory Project (NPP) satellite uses solar- and IR-based retrieval algorithms for cloud-top parameters and cloud optical properties that follow the fundamental principles of the heritage AVHRR and MODIS algorithms [11]–[15].

A few cirrus cloud remote sensing programs based on Atmospheric Infrared Sounder (AIRS) thermal IR window (TIRW) data have been developed, e.g., [16]–[18]. In particular, a thin cirrus cloud thermal IR RTM has been constructed for application to the remote sensing of thin cirrus clouds [19]. This radiation model combines the operational Optical Transmittance

Manuscript received August 18, 2011; revised March 27, 2012; accepted June 3, 2012.

S. S. C. Ou, K. N. Liou, and Y. Takano are with the Joint Institute for Regional Earth System Science and Engineering, University of California, Los Angeles, CA 90095 USA (e-mail: ssou@atmos.ucla.edu; knliou@atmos.ucla.edu; ytakano@atmos.ucla.edu).

B. H. Kahn and Q. Yue are with the Jet Propulsion Laboratory, California Institute of Technology, Pasadena, CA 91109 USA (e-mail: brian.h.kahn@jpl.nasa.gov; Qing.Yue@jpl.nasa.gov).

M. M. Schreier is with the Joint Institute for Regional Earth System Science and Engineering, University of California, Los Angeles, CA 90095 USA, and also with the Jet Propulsion Laboratory, California Institute of Technology, Pasadena, CA 91109 USA (e-mail: mathias.schreier@jpl.nasa.gov).

Color versions of one or more of the figures in this paper are available online at http://ieeexplore.ieee.org.

Digital Object Identifier 10.1109/TGRS.2012.2205261

(OPTRAN) model [20] and a thin cirrus cloud parameterization using a number of observed ice crystal size and shape distributions. Previous numerical simulations [21], [22] show that cirrus cloudy radiances in the 800–1130-cm^{-1} TIRW are sufficiently sensitive to variations in cirrus optical depth (τ_c) and small ice crystal mean effective diameter ($D_e < 50$ μm), as well as in ice crystal shape, if appropriate shape distribution models are selected *a priori* for analysis. The thin cirrus thermal IR RTM is based on the delta-four stream (D4S) approximation [24], [25], which accounts for ice crystal scattering to facilitate high-spectral-resolution remote sensing of cirrus cloud τ_c in AIRS data. The aforementioned retrieval methodologies [19], [23] are applicable to AIRS data, but the issue of speed versus accuracy must be addressed, particularly with regard to the minimization approach.

All the aforementioned AIRS cirrus cloud retrieval programs are time consuming. To investigate the problem of computational speed, a new cirrus cloud retrieval method based on a k-coefficient approach using AIRS cloud-cleared radiances (ACCRs) at AIRS/Advanced Microwave Sounding Unit (AMSU) resolution as input has been developed. To facilitate a more rapid retrieval using cloud-cleared radiances, a novel k-coefficient cloud retrieval approach that separates clear and cloudy radiances has been developed. This approach follows up the heritage of the two-channel TIRW (3.7 and 10.9 μm) correlation method [3], which has been applied to AVHRR data with validation using collocated *in situ* and ground-based lidar and radar measurements [26]–[31]. The two-channel TIRW method has been implemented in the NPP cloud retrieval chain for retrieving both daytime and nighttime cirrus cloud parameters [11], [13]–[15]. In the present approach, the cirrus cloudy radiance in the TIRW region is expressed as the sum of the cloud emission and the transmitted below-cloud upwelling radiance, which can be approximated by cloud-cleared radiance due to negligible above-cloud water vapor emission/absorption.

This new approach has been tested against a more accurate retrieval program which combines the D4S program with an accurate and computationally efficient RTM, the Stand-alone AIRS Radiative Transfer Algorithm (SARTA) [32]. The SARTA is a narrow-band radiative transfer program and is used in the AIRS physical retrieval program. It is specifically designed to simulate clear-sky upwelling radiance at the top of the atmosphere (TOA) for any given AIRS channel and atmospheric profile. It effectively parameterizes atmospheric transmittances in 100 pressure layers using the AIRS spectral response functions measured during prelaunch testing [32], [33]. This radiative transfer program includes surface and atmospheric emission/absorption, as well as surface reflected thermal and solar radiation terms.

The D4S for IR radiative transfer has been discussed in detail [34]. It accounts for scattering/emission interaction within each cirrus cloud layer based on prescribed ice crystal single-scattering property models. For the execution of D4S, we have incorporated the most updated high-resolution ice crystal microphysics and thermal IR optical properties developed by the MODIS algorithm group [35]. The TOA AIRS spectral radiances for skies containing cirrus are evaluated by convolving the clear-sky transmittances from SARTA and cloudy layer transmittances/reflectances from D4S. Based on the SARTA+D4S radiative transfer program, a cirrus cloud retrieval scheme using a lookup-table approach was developed. To demonstrate the performance of the retrieval method, it is applied to a number of AIRS granules that contain cirrus clouds. Recently, a fast IR RTM [36] based on a radiance-tracing principle for overlapping cloudy conditions and a more accurate IR RTM [37] based on the adding–doubling approach have been developed.

The SARTA+D4S radiative transfer program is an accurate method for the computation of AIRS cirrus cloudy spectra for remote sensing applications. However, in the retrieval, the SARTA model has to be repeatedly executed for each atmospheric temperature/humidity profile associated with the AMSU footprint. For efficient operational retrievals, it is desirable to reduce computations of atmospheric transmittance and gaseous optical depths, and instead replace them with cloud-cleared radiances, e.g., [38]. In the SARTA+D4S retrieval implementation, cloudy (D4S) and clear (SARTA) transmittances are convolved to produce cloudy radiances, and the retrieval cannot be modified to incorporate cloud-cleared radiances.

The present approach fundamentally differs from previous AIRS thermal IR retrieval/simulation approaches [16], [17], [22], [23] in five aspects.

1) *Clear radiance*. Clear radiances in previous AIRS thermal IR retrieval/simulation approaches have been computed through clear-sky transmittances from a line-by-line radiative transfer program [22], [39], SARTA [16], [17], or OPTRAN [19], [23]. A method of AIRS cloud retrievals directly using ACCRs has not been published to date. According to Susskind *et al.* [38], the AIRS cloud-clearing algorithm, as currently implemented, does not generate cloud optical properties as a by-product.
2) *Cloud radiative transfer program*. Another significant improvement is that an efficient k-coefficient parameterization coupled with the D4S method is used. To date, scattering effects for cirrus clouds with low and moderate optical depths have been accounted for by the accurate, yet computationally inefficient, discrete ordinate RTM [22], a radiance-tracing parameterization approach [16], [17], a single-scattering approximation [19], and the D4S [23].
3) *Microphysics and single-scattering models*. Instead of using the simplified Henyey–Greenstein phase function [16], [17] or complicated size and shape models [19], [23], we used the most updated ice crystal single-scattering property models [35].
4) *Reduction of the number of spectral channels*. Previously developed AIRS retrieval programs employed a large number of cloud retrieval channels, sometimes numbering in the 100s. Notably, these programs employed a 790–970-cm^{-1} spectral region and used a slope method to determine the effective particle size. The present cloud retrieval program employs six AIRS channels characterized by minimal water vapor absorption/emission between 766 and 832 cm^{-1} and is demonstrated to be sensitive to both cirrus τ_c and D_e.

5) *Operational applicability*. In contrast to the cumbersome clear and cloudy radiative transfer calculations and the use of hundreds of cloud retrieval channels in previous approaches, the combination of the novel and computationally efficient k-coefficient approach with a direct use of cloud-cleared radiances makes the retrieval program potentially more suitable for operational applicability.

Overall, our purpose for developing a new RTM and parameterization is to show various possible approaches that balance the needs of accuracy, precision, and computational speed. Our primary objective is to construct an operationally feasible retrieval program with optimal efficiency and accuracy, utilizing cloud-cleared spectral radiances coupled with a fast cloud radiative transfer program.

II. k-Coefficient Cirrus Cloud Retrieval Method

The theoretical basis of the k-coefficient cirrus cloud retrieval program has been previously established [3], [11]. Here, we modify the retrieval methodology to be applicable to multiple channels. From the theory of radiative transfer, the upwelling radiance at TOA may be expressed for the six selected "clean" channels in terms of the cirrus cloud-top temperature T_c and emissivities ε_n as follows:

$$R_n = (1-\varepsilon_n)R_{an} + \varepsilon_n B_n(T_c), \qquad n = 1-6 \tag{1}$$

where R_{an} denotes the upwelling radiance reaching the cloud base for the six spectral bands and $B_n(T_c)$ is the respective Planck function at T_c. The first term on the right-hand side of (1) represents the contribution of the transmitted radiance from below the cloud, and the second term denotes the emission contribution from the cloud itself. The emission by water vapor above the cirrus cloud has been neglected. Effects of cloud reflectivity, which are generally less than 3% of the incident radiance based on exact radiative transfer calculations, have also been neglected. It must be pointed out that (1) is best applicable to "clean" TIRW wavelengths, where the cloud-base upwelling radiance can be approximated by the TOA clear radiance because of the negligible above-cloud absorption/emission. For each selected channel n

$$\varepsilon_n = 1 - \exp(-k_n\tau). \tag{2}$$

The exponential term represents the effective transmissivity. The parameter k_n represents the effective extinction coefficients for the six channels accounting for the effects of multiple scattering within cirrus clouds and for the ratios between visible and IR extinction coefficients. Generally, $k_n < 1$ because of the effect of multiple scattering. Thus, the products $k_n\tau$ may be considered as the effective optical depth that would yield the same emissivity values as for the pure absorption conditions.

By combining (1) and (2), we obtain

$$-\ln\left[\frac{R_n - B_n(T_c)}{R_{an} - B_n(T_c)}\right] = -\ln(1-\varepsilon_n) = k_n\tau_c. \tag{3}$$

We then define the residual that is to be minimized in order to solve for D_e and τ_c as

$$\chi_{ij} = \sum_{n=1}^{6}\left[-\ln(1-\varepsilon_n) - k_{nij}\tau_{ci}\right]^2 \tag{4}$$

where the subscripts i and j denote the index for reference τ_c and D_e, respectively.

In the two-channel (AVHRR 3.7 and 10.9 μm) method for retrieving cirrus cloud optical depth, particle size, and cloud temperature, a third equation, in addition to (1) and (2), must be added in order to close the equation system. To accomplish this, an empirical relationship between cloud temperature and cloud effective particle size had been introduced. In the current retrieval approach, since the number of equations is more than the number of unknowns, this relationship is no longer needed. The k-coefficient approach and the split-window approach [8] in PATMOS-x are similar. In the latter approach, IR emissivity is parameterized in terms of the 11–12-μm k-coefficient ratio, which, in turn, is evaluated based on the single-scattering approximation [40], while the current approach computes the k-coefficient for each channel computed based on the D4S approximation. Sensitivity study on the accuracy of retrieved cirrus cloud parameters has been performed in earlier works, e.g., [11].

III. SARTA+D4S, SARTA+k-Coefficient, and ACCR+k-Coefficient Approaches

To retrieve cloud optical properties, a radiative transfer parameterization (the k-coefficient approach) following (1) and (2) is used. To solve (1) for cloud optical properties, the clear radiance R_{an} must be determined beforehand. This parameter can be obtained either through SARTA computations using AIRS retrieved temperature and moisture profiles or directly from ACCRs. Because of SARTA's time-consuming nature, we use the ACCR. This cloud-cleared radiance is obtained neither by searching neighboring clear radiances nor by directly solving radiative transfer equations but by using both AMSU and AIRS data following a residual minimization method. In this paper, we test the new ACCR + k-coefficient approach against SARTA+D4S and SARTA + k-coefficient approaches.

The theoretical basis of the SARTA+D4S retrieval program is similar to that given in [19] and [23]. A cirrus layer is characterized by τ_c at $\lambda = 0.55$ μm and D_e, which are key parameters representing the scattering and absorption properties of a spectrum of ice crystal sizes and shapes. The thermal IR cirrus cloud optical depth τ_ν at a wavenumber ν can be derived via the relationship $\tau_\nu = \tau_c\langle Q_{ext,\nu}\rangle/2$, where $\langle Q_{ext,\nu}\rangle$ stands for the mean extinction efficiency for an AIRS channel. Assuming that each AIRS layer is homogeneous, the ice crystal transmission is convolved with gaseous transmission as follows: $\mathcal{T}_\nu = \mathcal{T}_{\nu,g}\cdot\mathcal{T}_{\nu,c}$, where $\mathcal{T}_\nu$ is the total transmittance at the cloud layer, $\mathcal{T}_{\nu,g}$ is the effective gaseous transmittance at a cloud layer computed from SARTA, and $\mathcal{T}_{\nu,c}$ is the cloud layer transmittance computed from D4S. Following Liou *et al.* [24], the delta-function adjustment has been applied to account for the forward diffraction peak in the four-stream radiative transfer approach to increase computational accuracy.

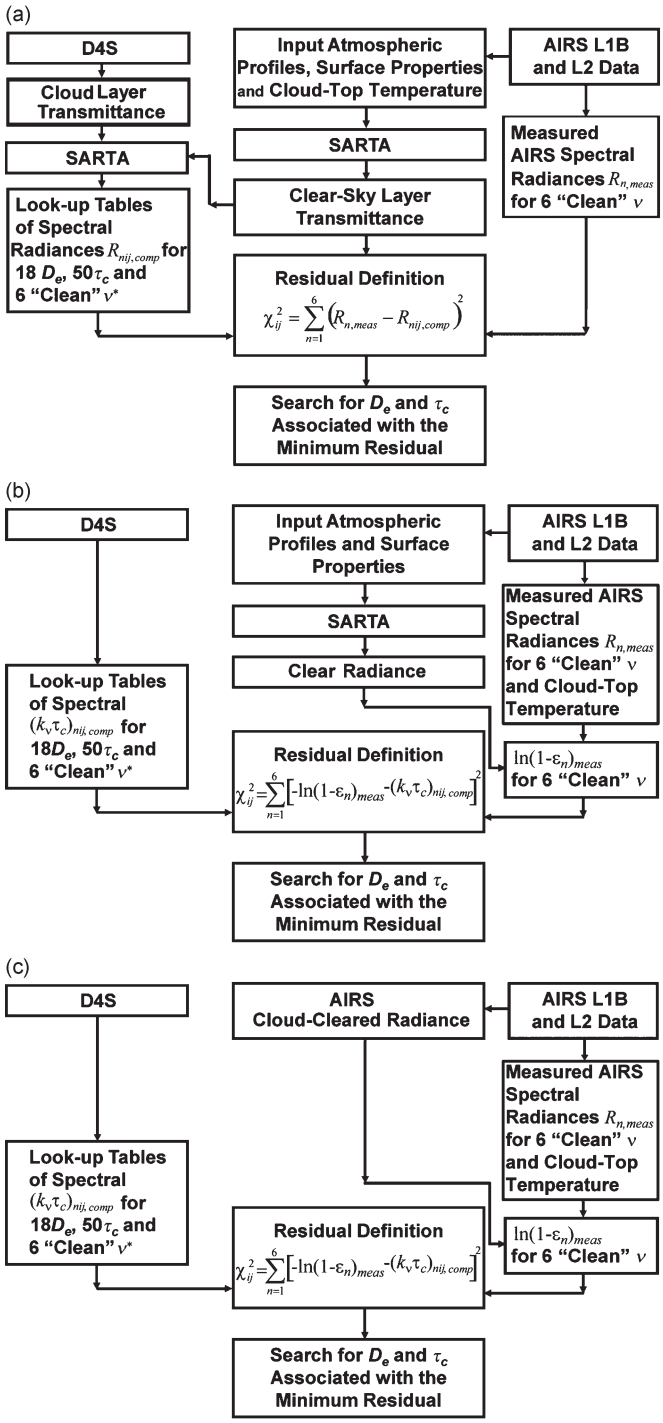

Fig. 1. (a) Flowchart of the SARTA+D4S retrieval program. (b) Flowchart of the SARTA + k-coefficient retrieval program. (c) Flowchart of the ACCR + k-coefficient retrieval program.

The SARTA+D4S retrieval program is illustrated by the flowchart shown in Fig. 1(a). The AIRS Level 1B (L1B) and Level 2 (L2) data sets are processed to generate input atmospheric temperature and humidity profiles and surface reflective and emissive properties in the radiance temperature profile data format. Cloud-top temperature is extracted from the AIRS L2 Standard product to represent the cirrus vertical location in the atmosphere, and a single-layer cloud is assumed herein, although in principle, it can be modified to include multiple cloud layers. To construct lookup tables, D4S is used to compute cloud transmittances for 50 reference τ_c's (between 0.2 and 10, $\Delta\tau_c = 0.2$) and 18 reference D_e's (between 10 and 180 μm, $\Delta D_e = 10$ μm) at the six selected channels. After convolving cloud transmittances with effective gaseous transmittances, the six-channel cirrus TOA spectral radiances are computed by using the SARTA. The six-channel residual, which is defined as the square sum of the difference between computed and measured radiances, is minimized with respect to τ_c and D_e to search for the solution of both cloud parameters that is associated with the minimum residuals. The procedure of minimization is similar to the steepest descent method [12] and is applied to cirrus clouds with optical depth less than 10.

The k-coefficient approach is implemented in two retrieval programs using different input clear radiances: 1) based on SARTA computations (SARTA + k-coefficient) and 2) based on ACCRs (ACCR + k-coefficient). These retrieval programs are illustrated by the flowcharts shown in Fig. 1(b) and (c). The SARTA + k-coefficient and SARTA+D4S programs follow the same procedure to generate spectral clear radiances R_{an}. In the ACCR + k-coefficient program, as shown in the flowchart of Fig. 1(c), we replace SARTA computed clear radiance with ACCR in the retrieval program.

The ice water path (IWP) is obtained from AIRS retrieval results of τ_c and D_e. To obtain a representative IWP, we have followed a parameterization approach [41] in which τ_c, IWP, and $r_e (= 1/2\, D_e)$ for cirrus clouds are related by the following equation:

$$\tau_c = IWP \left(e_0 + e_1/r_e + e_2/r_e^2\right) \tag{5}$$

where e_0, e_1, e_2 are the fitting coefficients, which are determined from thousands of ice crystal size distributions collected by airborne *in situ* sampling over midlatitude and tropical areas, along with the parameterization of the single-scattering properties using the data compiled by Liou *et al.* [42]. $IWPs$ are determined using the aforementioned parameterization for pixels that were identified as ice clouds based on the MODIS thermal IR cloud phase mask program.

IV. Cirrus Cloud Single-Scattering Properties

The cirrus cloud single-scattering properties, including single-scattering albedo (ω_0), asymmetry factor (g), and extinction efficiency (Q_{ext}), which are required for computing cloud layer transmittances, are computed based on a database for ice clouds [35]. This ice crystal size and shape database is designed for application to the retrieval of ice crystal properties in the midwave IR (2000–3250 cm^{-1}), IR (660–2000 cm^{-1}), and far IR (100 to 660 cm^{-1}) spectral regions, and the first two ranges encompass the AIRS spectral range. An ice crystal scattering property archive has been constructed for a variety of ice crystal shapes, including droxtals (approximating spheres), plates, hollow and solid columns, 3-D bullet rosettes, and aggregates. The database is based on a single size-dependent ice crystal shape mixture model. The database provides bulk single-scattering properties for 18 reference D_e's. No bulk ice crystal single-scattering phase function is needed in the D4S calculations since the D4S method only requires the g

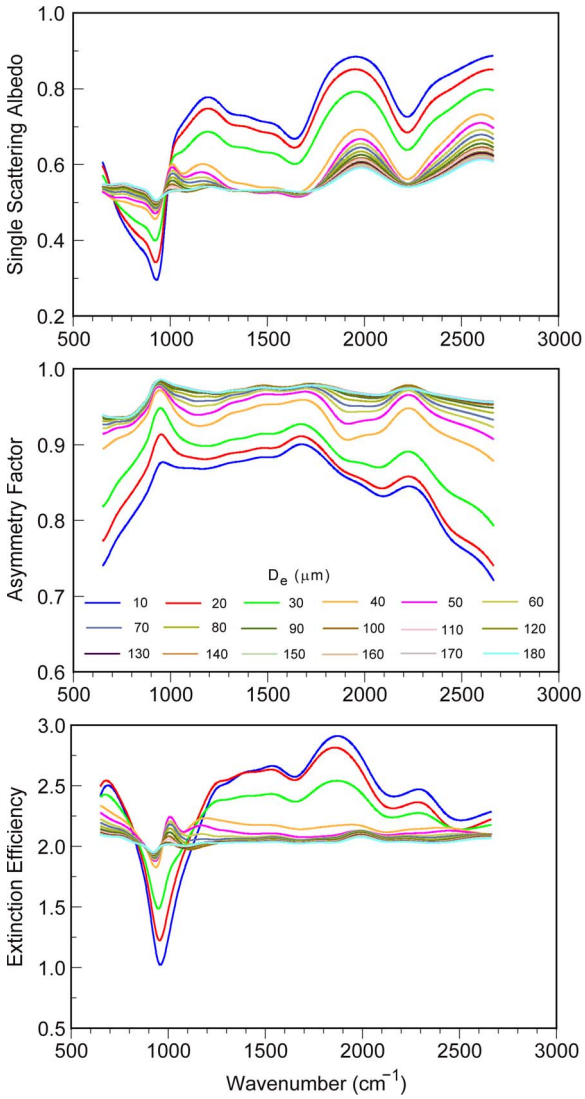

Fig. 2. (a) Single-scattering albedo, (b) asymmetry factor, and (c) extinction efficiency versus wavenumber from 500 to 3000 cm^{-1} as functions of the 18 reference D_e's.

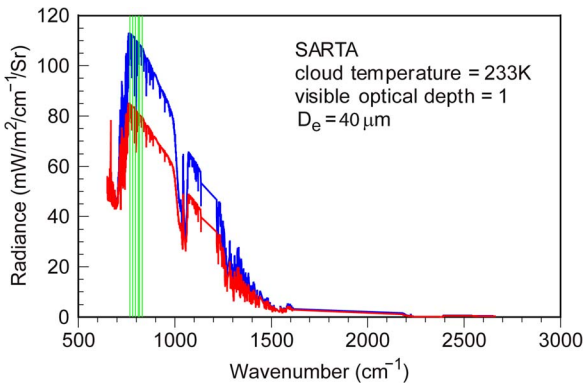

Fig. 3. (Blue color) Clear and (red color) cloudy spectra simulated by the SARTA+D4S program for a set of input temperature and humidity profiles that are close to the U.S. Standard climatological profiles with a cloud-top temperature of 233 K, $\tau_c = 1$, and $D_e = 40$ μm.

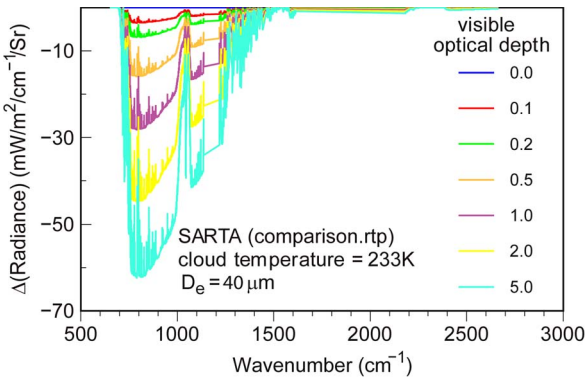

Fig. 4. Sensitivity of AIRS cloudy spectral radiances to τ_c in terms of the difference between clear and cloudy radiances $[\Delta R(\nu)]$ plotted versus the wavenumber as functions of optical depths with $D_e = 40$ μm and $T_c = 233$ K.

value. Linear interpolation has been applied in the wavenumber dimension to compute ice crystal single-scattering properties for the 2378 AIRS channel wavenumbers.

Fig. 2(a)–(c) shows ω_0, g, and Q_{ext} versus the wavenumber from 500 to 3000 cm^{-1} as functions of the 18 reference D_e's. It is noted that all three single-scattering parameters depend on the wavenumber and are sensitive to D_e. The plots contain a variety of spectral structure. It is also noted that ω_0 decreases with increasing D_e due to increased cloud particle absorption for $\nu > 1000$ cm^{-1}. However, for $\nu < 1000$ cm^{-1}, ω_0 increases with increasing D_e due to the dominating effect of Rayleigh scattering. The asymmetry factor g ranges between 0.7 and 0.98 and increases with increasing D_e subject to increasing fraction of forward scattering. The extinction efficiency Q_{ext} decreases with increasing D_e except for $800 < \nu < 1150$ cm^{-1}. The minima of ω_0 and Q_{ext} and the small peaks of g near 920 cm^{-1} are caused by the so-called Christiansen effect [43], [44]. At this wavenumber, the real part of the refractive index of ice approaches a minimal value (∼1.0873) so that the scattering effect is small, leading to minimum ω_0 and Q_{ext}, and the forward scattering (transmitted) fraction is increased, leading to a locally maximum g. The Christiansen effect is particularly prominent for smaller ice crystal sizes, and therefore, it results in the high sensitivity of ω_0 and Q_{ext} to D_e for wavenumbers between 700 and 1100 cm^{-1}.

The atmospheric temperature, water vapor and ozone profiles, and surface properties, including surface IR emissivity and reflectivity, are taken for input to the SARTA from the Version 5 (V5) AIRS L2 Standard and Support retrieval product data sets. Fig. 3 shows the clear (blue) and cloudy (red) spectra simulated by the SARTA+D4S program for a set of input temperature and humidity profiles that are similar to the U.S. Standard climatological profiles with a cloud-top temperature of 233 K, a visible τ_c of 1, and a D_e of 40 μm. Clear and cloudy spectra can differ by as much as 20 mW/m^2/cm^{-1}/sr for wavenumbers between 700 and 1000 cm^{-1}. Fig. 4 shows the sensitivity of AIRS cloudy spectral radiances to τ_c, where differences between clear and cloudy radiances $[\Delta R(\nu)]$ are plotted versus the wavenumber as functions of τ_c with $D_e = 40$ μm and $T_c = 233$ K. For a typical cirrus cloud ($\tau_c = 5$), $\Delta R(\nu)$ can reach as high as 60 mW/m^2/cm^{-1}/sr. There is a significant cloud sensitivity occurring near $\nu = 800$ cm^{-1} for $\tau_c = 1$, where the derivative $\Delta R(\nu)/\Delta\tau_c \sim -30$ mW/m^2/cm^{-1}/sr. The sensitivity is lower for strong water vapor absorbing channels ($\nu = 1300 - 2100$ cm^{-1}). Fig. 5 shows the sensitivity of AIRS cloudy spectral radiances to D_e, where the difference between cloudy

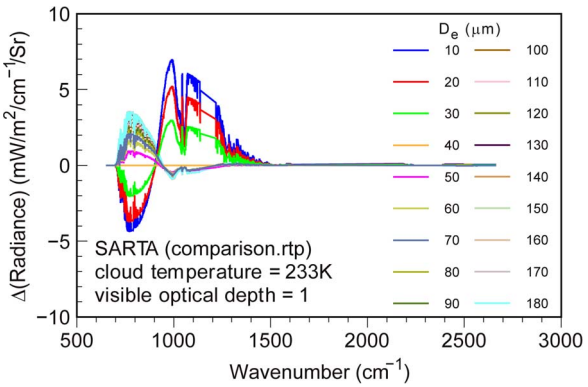

Fig. 5. Sensitivity of AIRS cloudy spectral radiances to D_e in terms of the difference between cloudy radiances for $D_e = 40$ μm and other D_e's plotted versus wavenumbers between 500 and 3000 cm^{-1} as functions of D_e with $\tau_c = 2$ and $T_c = 233$ K.

radiances for $D_e = 40$ μm and other D_e's are plotted versus the wavenumber between 500 and 3000 cm^{-1} as functions of D_e with $\tau_c = 2$ and $T_c = 233$ K. It is shown that $R(\nu)$ increases as D_e increases for 700 cm$^{-1} < \nu <$ 900 cm^{-1}, and $R(\nu)$ decreases as D_e increases for 900 cm$^{-1} < \nu <$ 1200 cm^{-1}. Peak cloud sensitivity occurs near $\nu = 800$ and 1000 cm^{-1}, where $\Delta R(\nu)/\Delta D_e \sim -0.06$ and $+0.06$ mW/m^2/cm^{-1}/sr/μm, respectively, which resemble the spectra shown in [22].

V. Selection of Retrieval Channels

For operational applicability, it is desirable to select the minimum number of channels with optimal retrieval accuracy.

In view of the fact that the slope of the IR brightness temperature spectrum between 790 and 960 cm^{-1} is sensitive to the effective particle size and that a strong sensitivity of the IR brightness temperature to cloud optical thickness is noted at wavenumbers between 1050 and 1250 cm^{-1} [22], we examined the sensitivity of spectral radiances to τ_c and D_e for these spectral regions based on simulation results from SARTA+D4S. Since Figs. 4 and 5 show that radiances for 760–840 cm^{-1} are sensitive to τ_c from 0 to 5 and to D_e between 10 and 180 μm, respectively, we choose to use radiances for 760–840 cm^{-1} to carry out retrievals. By examining the SARTA spectra for 760–840 cm^{-1}, we identified six channels: 766, 781, 795, 811, 817, and 832 cm^{-1}, which are characterized by minimal water vapor absorption/emission and high sensitivity to ω_0 and Q_{ext}, consequently sensitive to D_e, and their spectral locations are denoted by green vertical lines in Fig. 3. The minimal water vapor absorption is about the same for both 760–840 cm^{-1} and 1050–1250 cm^{-1}, and the CO_2 absorption for 760–840 cm^{-1} is also minimal [45].

Below, we demonstrate the effectiveness of using the six selected channels for the purpose of cloud retrievals. In the modified OPTRAN+single-scattering approach [46], 14 channels have been selected: 811, 817, 832, 843, 861, 873, 892, 899, 915, 961, 964, 1079, 1096, and 1127 cm^{-1}. The derivative of the brightness temperatures for these channels with respect to the wavenumber has been found to be sensitive to D_e, particularly for small ice crystals. We have executed the retrieval programs using both the 14-channel and the six-channel sets (totaling 17 channels, with three overlapping channels). Retrieval results show that the τ_c mean and root mean square (rms) differences are small (0.031 and 0.19), with a high correlation of coefficient of 0.987. However, the 17-channel retrieval produced less retrievable D_e's than the 6-channel approach, with a mean bias of about 3 μm and rms differences of 10 μm. These differences are presumably caused by the fact that radiances for 1050–1250 cm^{-1} are less sensitive to D_e for $D_e > 40$ μm. We will further investigate the inclusion of radiances for 1050–1250 cm^{-1} in our future application of the retrieval algorithm.

VI. Application to Air Granules Containing Cirrus

The similarities and differences between the SARTA+D4S, SARTA + k-coefficient, and ACCR + k-coefficient retrieval approaches are demonstrated with observed AIRS scenes. The Standard L2 cloud products, including cloud height, temperature, and cloud fraction [46]–[51], and the surface and atmospheric properties, such as temperature, water vapor, surface skin temperature, and emissivity [52], [53], have been the subject of many validation studies. Cirrus is identified based on the *ad hoc* threshold of $T_c < 243$ K, and a more detailed phase algorithm is under development [54], [55]. Also, retrieved τ_c and D_e are quantitatively compared with collocated MODIS retrieval products. Sensitivity studies on the performance of the k-coefficient method subject to uncertainty in the assumed cloud microphysics model have been performed and reported in earlier published works, e.g., [11].

A. Differences Between SARTA+D4S, SARTA+k-Coefficient, and ACCR+k-Coefficient

We start with the analysis of an Aqua overpass in Mongolia and North Central China on Oct 17, 2006, at 0617 Coordinated University Time (UTC) (AIRS Granule #63) and over Siberia at 0623 UTC (AIRS Granule #64). The MODIS true color [see Fig. 6(a) and (b)], 1.38-μm reflectance [see Fig. 6(c)], cloud phase mask [see Fig. 6(d)], and cloud-top temperature images [see Fig. 6(e)] for 0620 and 0625 UTC are collocated with AIRS granules #63 and #64, respectively. For 0620 UTC, the true-color image and the 1.38-μm reflectance maps show a few large patches of cirrus clouds in an east–west streaking pattern over the Inner Mongolia region, and a large area of cloudiness is present over North Central China. The MODIS cloud phase mask [see Fig. 6(d)] shows that the majority of cloudy pixels are cirrus clouds, consistent with the 1.38-μm cirrus cloud reflectance map. The cloud-top temperature maps [see Fig. 6(e)] for areas masked as opaque cirrus and mixed-phase clouds are generally lower than 220 and 240 K, respectively, further confirming that these areas contain cirrus clouds. For 0625 UTC, a large patch of stratiform clouds covers Central Siberia [see Fig. 6(b)]. The 1.38-μm reflectance [see Fig. 6(c)], cloud phase maps [see Fig. 6(d)], and preponderance of cloud-top temperatures < 240 K indicate that this patch is mostly opaque cirrus clouds with scattered mixed-phase clouds.

Fig. 7(a) shows an image of the AIRS channel 760 (11.1 μm; 900.562 cm^{-1}) brightness temperatures. The coastline of southern China, Hainan Island, and Bangladesh is shown near the

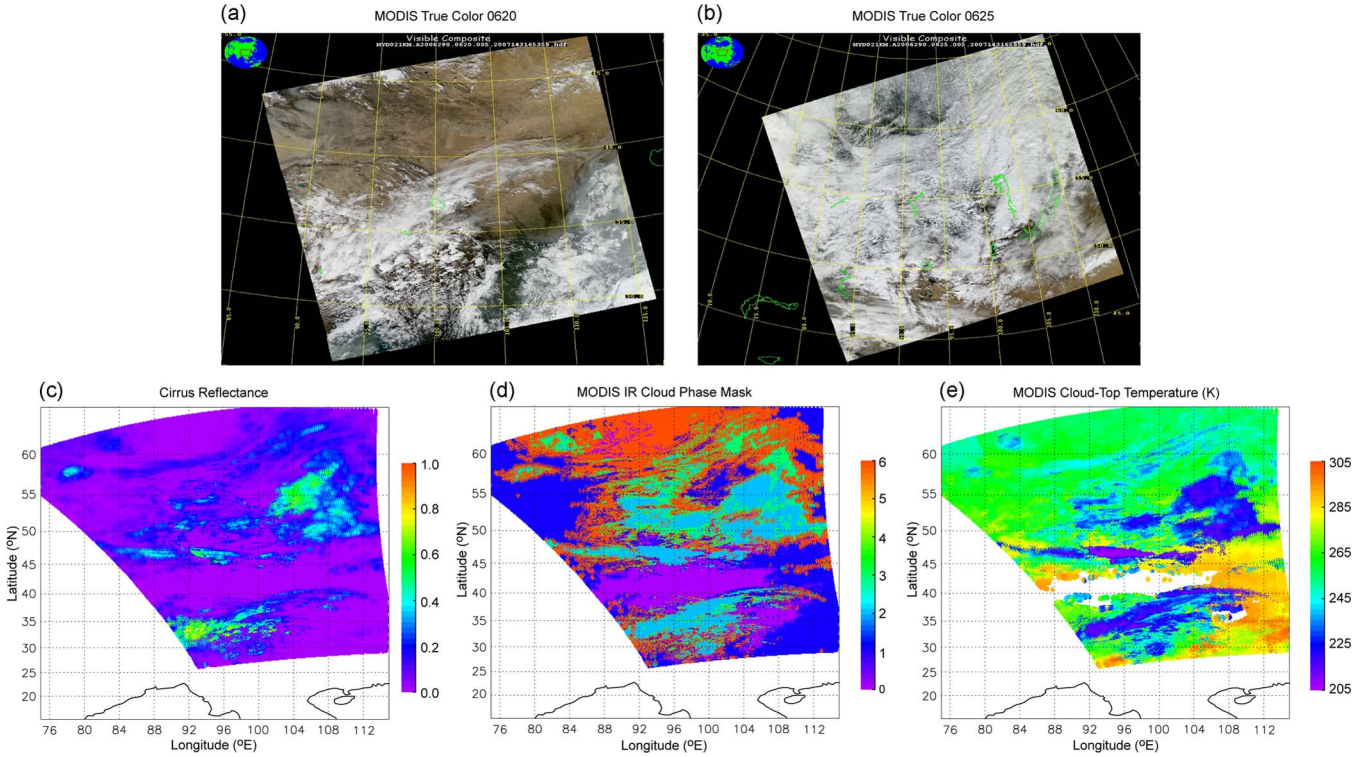

Fig. 6. (a) and (b) MODIS true color, (c) 1.38-μm cirrus cloud reflectance, (d) cloud phase mask, and (e) cloud-top temperature images for October 17, 2006, at 0620 and 0625 UTC collocated with AIRS granules #63 and #64. Cloud-type indices for (d) are the following: 0 = clear, 1 = opaque water cloud, 2 = opaque ice cloud, 3 = mixed-phase cloud, 4 = nonopaque ice cloud, 5 = nonopaque water cloud, and 6 = uncertain.

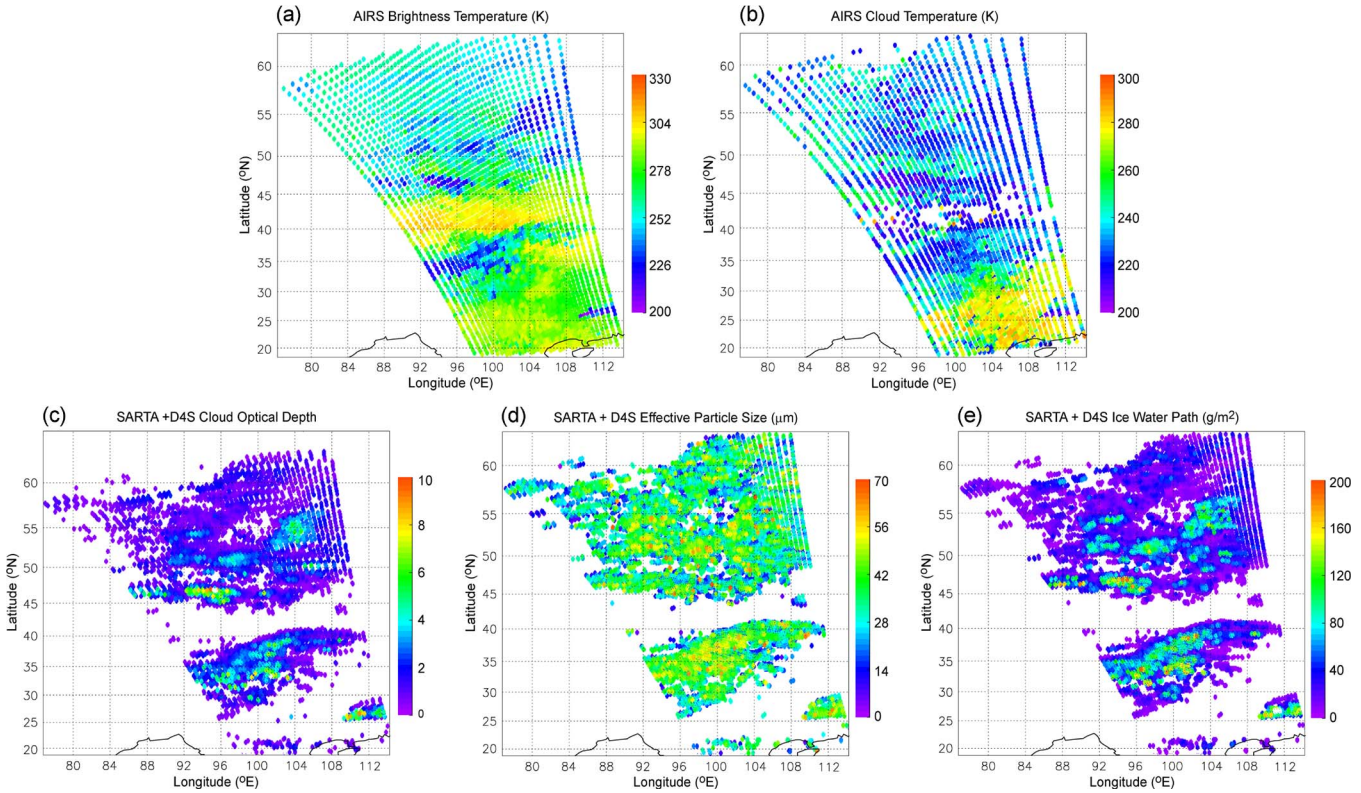

Fig. 7. (a) Image of AIRS channel 760 (11.1 μm; 900.562 cm^{-1}) brightness temperatures, (b) image of cloud-top temperature, and (c)–(e) SARTA+D4S retrieved τ_c, D_e, and IWP, respectively.

bottom of the image. The brightness temperature distribution shown in Fig. 7(a) is consistent with cloud patterns shown in Fig. 6. Fig. 7(b) shows the distribution of AIRS-derived cloud-top temperatures. The cloud-top temperatures are reported at AMSU resolution (V5). The data-void regions around 40–45° N and around 60° N are clear sky according to AIRS.

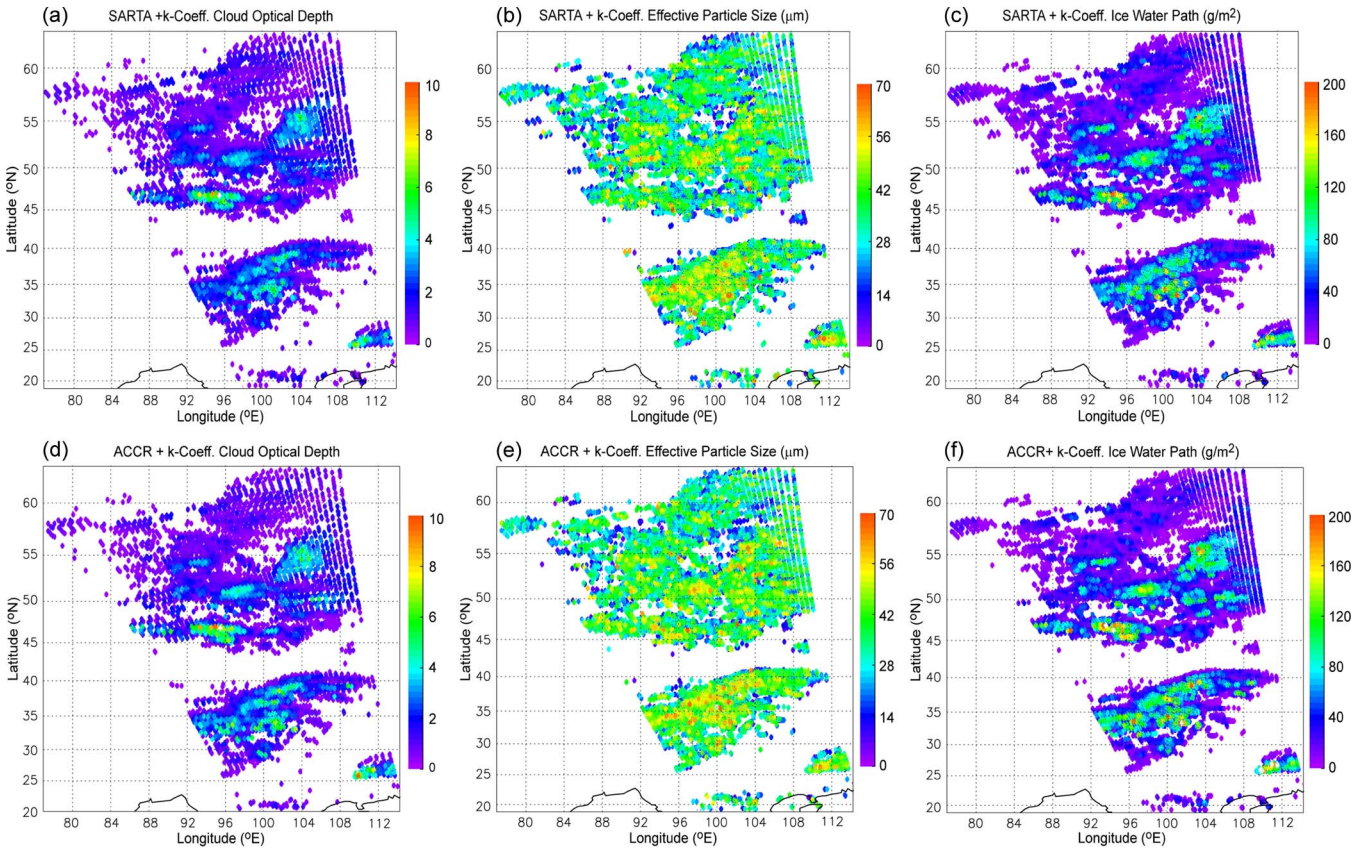

Fig. 8. (a)–(c) SARTA + k-coefficient retrieved τ_c, D_e, and IWP, respectively, and (d)–(f) the distribution of the same three cloud parameters as (a)–(c) from ACCR + k-coefficient retrievals.

Cloud-top temperatures for cloudy areas north of 30° N are generally lower than 240 K, confirming that these cloudy areas likely contain ice clouds (also see the MODIS phase mask). Cloudy areas south of 30° N are low clouds, except for a small patch near 112° E.

Fig. 7(c)–(e) shows the SARTA+D4S retrieved τ_c, r_e, and IWP, respectively. SARTA+D4S retrieves cloud parameters for footprints between 30° and 40° N and north of 45° N. The values of τ_c are mostly < 4, except for a few patches with τ_c as high as 7. The r_e's are mostly between 10 and 40 μm, with scattered larger values as high as 70 μm. The distribution of IWP is closer to that of τ_c than r_e with larger IWP values corresponding to larger τ_c values. For the cloud patch between 30 and 40° N, r_e's are smaller around cloud edges than cloud-center areas. Larger r_e's near the center of clouds correspond to larger τ_c. The $IWPs$ are mostly less than 60 g $\cdot$ m^{-2}, except for a few patches with associated $IWPs$ reaching as high as 120 g $\cdot$ m^{-2}. The maximum value of IWP reaches beyond 200 g $\cdot$ m^{-2} as shown for a few scattered footprints.

Fig. 8(a)–(c) shows the SARTA+k-coefficient retrieved τ_c, r_e, and IWP, respectively, and Fig. 8(d)–(f) shows the distribution of the same three cloud parameters from ACCR+k-coefficient retrievals. The distribution pattern and the range of cloud parameters are very similar to those from SARTA+D4S retrievals shown in Fig. 7(c)–(e). However, differences exist between images of the same cloud parameter due to uncertainties in the parameterized cloudy radiances from the k-coefficient approach and in the cloud-cleared radiances. To further compare the performance of the three retrieval programs, Fig. 9(a)–(c) shows the scatter plots of SARTA+k-coefficient versus SARTA+D4S retrieved cloud parameters, and Fig. 9(d)–(f) shows the scatter plots of ACCR+k-coefficient versus SARTA+k-coefficient retrieved cloud parameters. Correlations for τ_c, r_e, and IWP between the three approaches are characterized by small mean and rms differences. Between the SARTA+D4S and SARTA + k-coefficient approaches, mean differences for τ_c, r_e, and IWP are 0.0884 ($\sim$2%), 0.129 μm ($\sim$0.4%), and -1.37 g $\cdot$ m^{-2} (~ -1%), respectively, and these are very small differences. However, the rms differences for the three cloud parameters in the same order are 0.428 ($\sim$10%), 7.39 μm ($\sim$25%), and 11.5 g $\cdot$ m^{-2} ($\sim$12%). These larger rms values are caused by differences between the cloudy radiances simulated by the SARTA+D4S and SARTA + k-coefficient programs. Between the SARTA + k-coefficient and ACCR + k-coefficient approaches, the mean differences for τ_c, r_e, and IWP are 0.0285 ($\sim$0.7%), -0.2 μm (~ -0.7%), and 1.38 g $\cdot$ m^{-2} (~ -1%), respectively. However, the rms differences for the three cloud parameters in the same order are 0.405 ($\sim$10%), 15.9 μm ($\sim$50%), and 20.8 g $\cdot$ m^{-2} ($\sim$20%). These rms values reflect the differences between SARTA-simulated and cloud-cleared radiances obtained during the AIRS retrieval [56].

The scatter plots for τ_c and r_e have the highest and lowest correlations, respectively. Fig. 9(a) and (d) shows that the

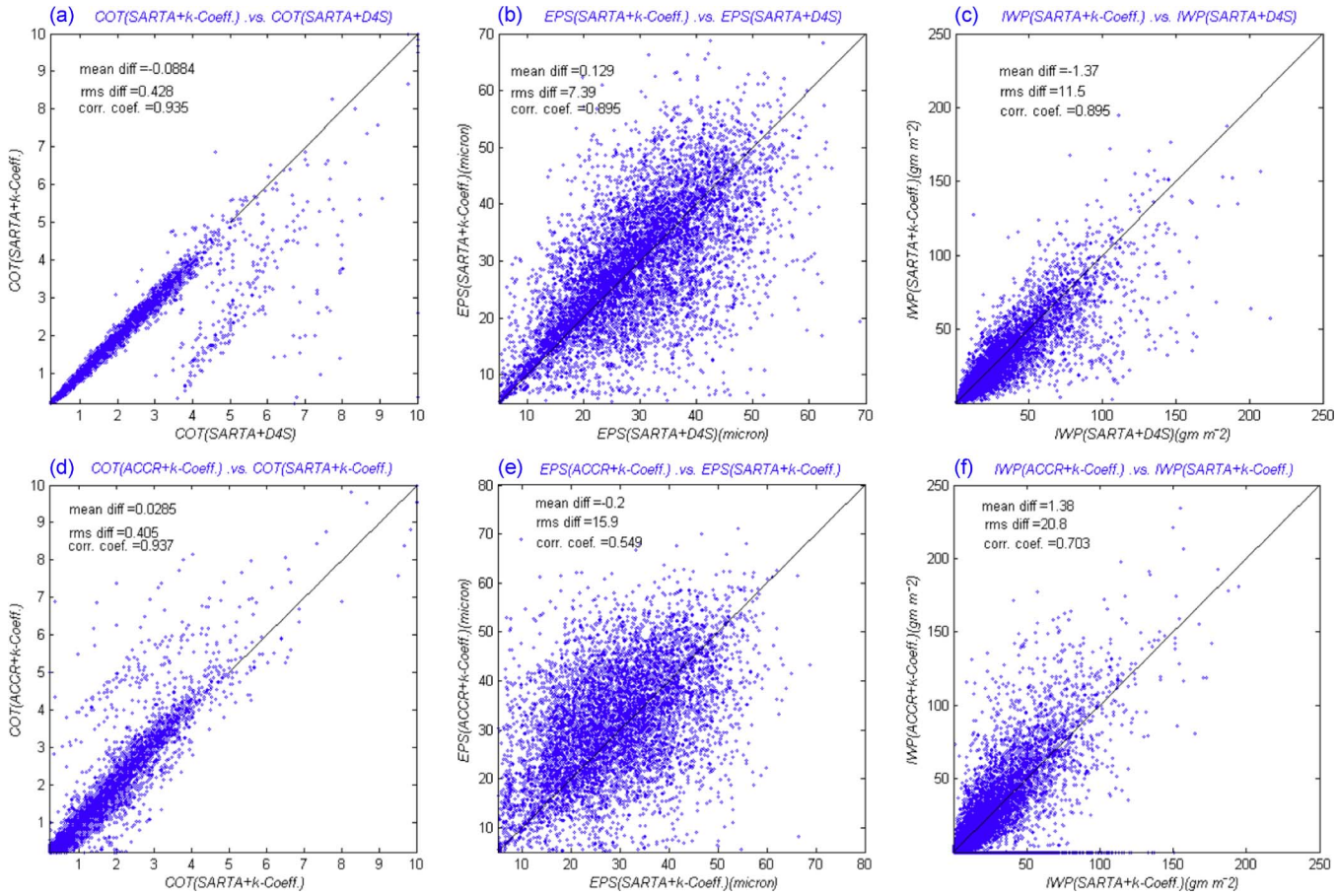

Fig. 9. (a)–(c) Scatter plots of SARTA + k-coefficient versus SARTA+D4S retrieved τ_c, D_e, and IWP and (d)–(f) scatter plots of ACCR + k-coefficient versus SARTA + k-coefficient retrieved cloud parameters. COT and EPS in the labels denote τ_c and D_e, respectively.

correlation coefficient is high ($\sim$0.94) for τ_c, while Fig. 9(b) and (e) shows lower correlation coefficients for D_e. This behavior is expected since the spectral radiances for the six selected channels are more sensitive to τ_c than to r_e. As discussed earlier, the peak $\Delta R(\nu)/\Delta\tau_c$ is approximately -30 mW/m^2/cm^{-1}/sr, but the peak $\Delta R(\nu)/\Delta D_e$ is approximately -0.06 /m^2/cm^{-1}/sr/μm at 800 cm^{-1}. Therefore, the same differences in simulated radiances lead to better correlation in retrieved τ_c than in r_e. The correlation coefficients for IWP are in between those for τ_c and r_e. The retrieval performance of other AIRS granules has also been examined, and results are nearly identical as those shown in Fig. 9. Overall, Fig. 9 shows that the faster k-coefficient method using cloud-cleared radiances as input can achieve an accuracy comparable to that of the more time-consuming SARTA+D4S method. The retrievals from the faster k-coefficient method may be "noisier," but the scatter is essentially Gaussian. This pattern will facilitate the compilation of a long-term cloud climatology. It is estimated that the SARTA+D4S and SARTA + k-coefficient approaches consume about the same amount of CPU time ($\sim$1 s per 3 $\times$ 3 AIRS footprints on a Silicon Mechanics workstation with an Intel 2.66-GHz processor), but the ACCR + k-coefficient approach is faster than the two approaches by about 10% CPU time. This reduction may seem small. However, we suspect that the potential reduction may actually be larger if the cloud scattering and retrieval computations are optimized since these components are much more time consuming than the clear-sky SARTA calculation.

B. Comparison With MODIS and CALIPSO/CloudSat Results

Having shown the consistency between the three retrieval approaches, we will demonstrate the accuracy of the ACCR + k-coefficient approach. AIRS retrieval results were compared with collocated MODIS/Aqua cloud products. Fig. 10(a) and (b) shows the images of filtered ACCR + k-coefficient retrieved τ_c and r_e, and Fig. 10(c) and (d) shows the images of filtered MODIS cloud parameters. To obtain these images, the MODIS granules are collocated to AIRS granules, and MODIS cloud parameters are averaged over collocated AIRS footprints using the methodology of Schreier *et al.* [57]. Our validation effort focused on the comparison of retrieved cloud parameters for footprint-overcast semitransparent optically thin cirrus clouds, so the effect of partial cloudiness within the AIRS footprint is minimal. For this reason, we have filtered out collocated AIRS and MODIS footprints for which MODIS cloud fraction $<$80%, $\tau_c > 10$, and $T_c > 243$ K. For a partially cloudy AIRS footprint, the MODIS τ_c is based on averaging the τ_c of MODIS cloudy pixels.

Fig. 10(a) and (c) shows that AIRS τ_c's are mostly smaller than MODIS values. Possible explanations for this difference are given hereinafter. Collocated MODIS and CALIPSO cirrus

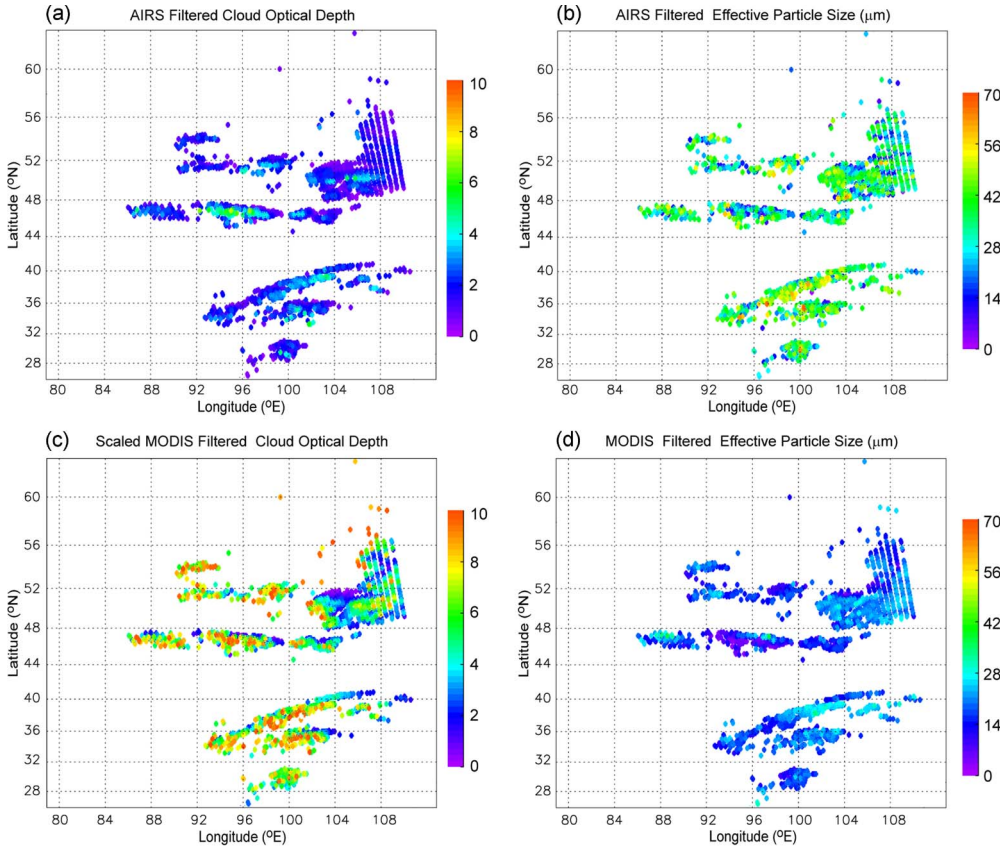

Fig. 10. (a) and (b) Filtered ACCR + k-coefficient retrieved τ_c and D_e. (c) and (d) Same as (a) and (b) except for cloud parameters from MODIS cloud product.

τ_c's have been compared, and MODIS archived τ_c's are about twice as large as CALIPSO values for thin cirrus clouds [58]. Currently, investigations on the cause of this difference are in progress. The CALIPSO τ_c may be biased low given the uncertainty in the multiple scattering factor [59]. On the one hand, filtered MODIS footprints may still contain effects of underlying low clouds that cause a high τ_c bias. On the other hand, because the relationship between spectral radiances and τ_c is nonlinear [60], the AIRS τ_c may be smaller than the arithmetically averaged MODIS τ_c within the collocated AIRS footprint. It is also possible that, for AIRS footprints with MODIS cloud fraction less than 100%, the AIRS τ_c may be biased lower due to the contribution of clear-sky radiance. Finally, for the condition of high semitransparent ice cloud overlying low-level water cloud, the true τ_c for the upper ice cloud can be obtained by replacing R_{an} by the Planck function $B_n(T_{cb})$ in (3), where T_{cb} is the cloud-top temperature of the low cloud [27]. Thus, AIRS τ_c based on (3) using R_{an} could be biased higher. However, we expect this bias to be small because, for a large part of multilayer cloudy conditions, the low-level clouds are stratus which are close to the surface, implying that $B_n(T_{cb})$ is close to R_{an} [61]. The domain-mean MODIS τ_c (5.0) is more than twice as large as the AIRS mean value (1.9).

After filtering out heterogeneous AIRS pixels, the AIRS r_e (mean $= 30.2$ μm) is shown to be larger than MODIS/Aqua values (mean $= 21.3$ μm). A possible reason for this difference may arise due to the fact that AIRS samples the midcloud region and MODIS/Aqua samples the upper portion of the cloud [62].

TABLE I
MEAN AND RMS DIFFERENCES AND CORRELATION COEFFICIENTS FOR AIRS AND MODIS COMPARISON OF τ_c AND r_e FOR OCTOBER 17, 2006 AT 0617 UTC (SCENE A) AND OCTOBER 23, 2007 AT 0515 UTC (SCENE B)

Scene	Cloud parameters	Mean Diff	RMS Diff	Corr. Coeff.
A	τ_c	-3.1	3.7	0.89
	$r_e(\mu m)$	8.9	9.7	0.80
B	τ_c	-3.5	4.1	0.61
	$r_e(\mu m)$	9.5	11.3	0.8

For typical cirrus clouds, D_e's are stratified with cloud-top values typically smaller than cloud-base values. It is also demonstrated that, by analyzing three MODIS cases and employing the differential absorption characteristics of MODIS 1.64, 2.13, and 3.75 μm band reflectances, the averages of the retrieved cloud-top and cloud-base r_e's, approximating midcloud values, are, in general, larger than MODIS r_e by 0–30 μm.

We have examined additional two AIRS granules (#52 and #53) for the MODIS/Aqua flight over Northeast Asia around 0515 UTC on Oct 23, 2007. The MODIS true-color composite image and cloud mask result displays a large area of stratiform cirrus clouds over Eastern Siberia. We have compared AIRS and MODIS retrieved τ_c and r_e subject to the same filtering procedure as described earlier. As in the case of October 17, 2006, the domain-mean MODIS τ_c (5.0) is more than twice as large as the AIRS mean value (1.54), while the AIRS r_e

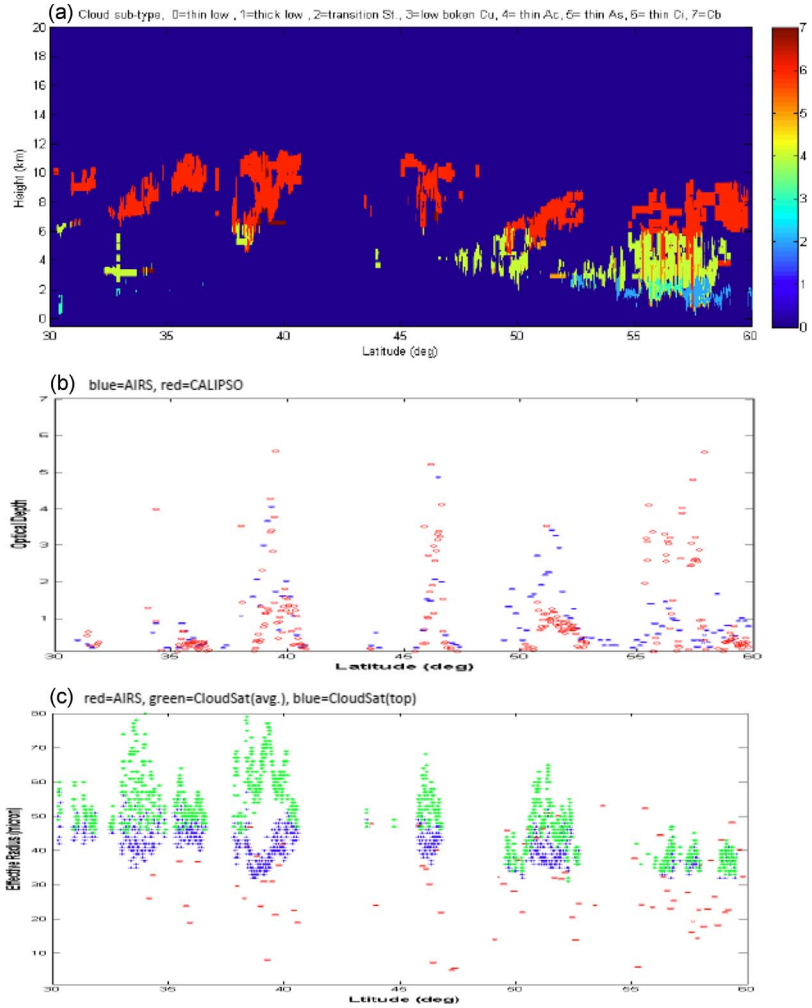

Fig. 11. (a) Result of cloud-type mask derived from the vertical feature mask obtained from Cloud-Aerosol Lidar with Orthogonal Polarization/CALIPSO polarized echoes. Cirrus clouds are identified as red. (b) Comparison of (blue) AIRS and (red) CALIPSO column optical depths. (c) Comparison of (red) AIRS r_e with CloudSat (green) vertically averaged and (blue) cloud-top r_e.

(mean $= 39.2$ m) is shown to be larger than MODIS/Aqua values (mean $= 29.6$ m). Table I gives the mean and rms differences and correlation coefficients for AIRS and MODIS comparison of τ_c and r_e for October 17, 2006 at 0617 UTC (Scene A) and October 23, 2007 at 0515 UTC (Scene B). For each scene and each cloud parameter, the rms difference is a little larger than the mean difference. Note that the correlation coefficients are all above 0.6, indicating that, although there are some differences between AIRS and MODIS retrieved cloud parameters, the two retrievals are well correlated.

The AIRS retrieval results were also compared with collocated CALIPSO and CloudSat cloud products. Fig. 11(a) shows the result of cloud-type mask versus latitude derived from the vertical feature mask obtained from CALIPSO polarized echoes. Cirrus clouds (red) are identified using the lidar depolarization technique. The cloud-type mask result indicates that there are thin cirrus clouds from 32° N to 40° N and from 45° N to 60° N between 6 and 12 km. Fig. 11(b) shows the comparison between the AIRS and CALIPSO retrieved τ_c's; the latter is extracted from the CALIPSO Level 2 5-km version 3.01 data product. The AIRS τ_c compare well with the CALIPSO τ_c for single-layer cirrus clouds from 32° N to 40° N and from 45° N to 53° N. However, the AIRS τ_c's are generally smaller than the CALIPSO τ_c from 55° N to 60° N, where the cloud-type mask shows cirrus clouds overlapping low-level clouds. Fig. 11(c) shows the comparison between the AIRS and CloudSat retrieved vertically averaged and cloud-top r_e's. The vertically resolved cloud effective particle sizes derived from the cloud profiling radar (CPR) backscatter data have been archived in the 2B-CWC-RO data product, where "CWC-RO" means Radar-Only Cloud Water Content. The AIRS r_e's are generally smaller than both sets of CloudSat r_e. There are two reasons for these differences. The first is that the Cloud Profiling Radar on board CloudSat tends to detect moderately thick cirrus with large cloud particle sizes [63], and the second is the AIRS retrieval uncertainty due to the averaging effect of the larger AIRS footprint.

VII. Summary and Conclusion

We have developed a cloud-radiative transfer program that combines D4S radiative transfer module with the currently operational SARTA, designed both for accuracy and computational efficiency of AIRS geophysical retrievals. The most

updated high-resolution ice crystal microphysics and thermal IR optical properties have been incorporated. Based on the SARTA+D4S radiative transfer program, a cirrus cloud retrieval scheme was developed using a lookup-table method and a residual minimization scheme. To directly use ACCRs so that repeated executions of SARTA can be skipped during retrieval processing, an alternative k-coefficient approach was developed based on radiative transfer parameterizations.

The theoretical basis of the k-coefficient retrieval program has been established. The retrieval methodology was modified to be applicable to multiple hyperspectral AIRS channels. Six AIRS channels were selected with minimal water vapor absorption/emission between 766 and 832 cm^{-1}. Spectral radiances for these channels are shown to be sensitive to τ_c and D_e. For each selected channel, the thermal IR emissivity is parameterized in terms of τ_c and a parameter k, which represents the effective extinction coefficients accounting for the effects of multiple scattering within cirrus clouds and for the ratios between visible and IR extinction coefficients.

The capability of SARTA+D4S, SARTA + k-coefficient, and ACCR + k-coefficient approaches is demonstrated by using AIRS L1B and L2 data sets. A case of AIRS/MODIS/Aqua overflight over North Central China and Mongolia on October 17, 2006 at 0617–0625 UTC is analyzed, covering two AIRS granules, where a few large patches of cirrus clouds for study were identified by examining both AIRS and collocated MODIS images. The SARTA+D4S retrieved τ_c, D_e, and IWP images show that reasonable values are obtained in this scene.

The distribution pattern and the range of cloud parameters from both SARTA + k-coefficient and ACCR + k-coefficient approaches are very similar to those from SARTA+D4S retrievals, with differences due to uncertainties in the parameterized cloudy radiances from the k-coefficient approach and in the cloud-cleared radiances. Scatter plots of results from the three approaches indicate good correlations between the approaches for all cloud parameters. The coefficients of correlation for τ_c are higher than for D_e since the spectral radiances for the selected six channels show better sensitivity to τ_c than to D_e. Optimal channel choices based on information theory principles that maximize sensitivity to effective diameter and optical thickness, e.g., [64], warrant further investigation.

We also demonstrate the operational applicability of the ACCR + k-coefficient approach by selectively comparing its retrieval results with collocated MODIS/Aqua, CALIPSO, and CloudSat thin cirrus cloud products. The distribution patterns of AIRS and MODIS τ_c's are qualitatively similar, with AIRS τ_c generally smaller than MODIS values, and AIRS r_e's are generally larger than MODIS/Aqua values. Reasons for these differences were discussed. AIRS retrieved τ_c's for a few of the areas of thin cirrus are comparable with CALIPSO τ_c, and AIRS retrieved r_e is lower than that of CloudSat, which is expected since the CPR tends to miss small cloud particles.

Overall, the present study gives the most detailed comparison to date on various AIRS retrieval approaches, including SARTA+D4S, SARTA + k-coefficient, and ACCR + k-coefficient methods, and it also quantifies the balance between accuracy and efficiency, as compared with previously developed approaches, which are more focused on sensitivity studies with demonstrations of operational applicability. Moreover, no one has presented a method of AIRS cloud retrievals using cloud-cleared radiances. The present study demonstrates that the ACCR + k-coefficient approach is a reliable alternative, which takes advantage of the available cloud-cleared AIRS radiances, reduces computational expense, and offers an efficient and reasonably accurate cirrus cloud retrieval alternative for hyperspectral IR observations. For the generation of an accurate climate data record, the SARTA+D4S is a very good tool. However, for the generation of a long-term global cloud climatology, the ACCR + k-coefficient approach may offer an important advance.

ACKNOWLEDGMENT

The authors Ou and Kahn would like to acknowledge the support for this work on behalf of the Atmospheric Infrared Sounder (AIRS) project at the Jet Propulsion Laboratory (JPL). Kahn and Schreier were partially supported by National Aeronautics and Space Administration Award NNX08AI09G. AIRS data were obtained through the Goddard Earth Sciences Data and Information Services Center (http://disc.gsfc.nasa.gov/). Moderate Resolution Imaging Spectroradiometer data were obtained through the Moderate Resolution Imaging Spectroradiometer Data Processing System (MODAPS) (http://ladsweb.nascom.nasa.gov/). CloudSat data were obtained through the CloudSat Data Processing Center (http://www.cloudsat.cira.colostate.edu/). CALIPSO Level 1B data were obtained through the Atmospheric Sciences Data Center at NASA Langley Research Center (http://eosweb.larc.nasa.gov/). A portion of this work was performed within the Joint Institute for Regional Earth System Science and Engineering of the University of California at Los Angeles, Los Angeles, and at the JPL, California Institute of Technology, under a contract with NASA.

REFERENCES

[1] T. Nakajima and M. D. King, "Determination of the optical thickness and effective particle radius of clouds from reflected solar radiation measurements. Part I: Theory," *J. Atmos. Sci.*, vol. 47, no. 15, pp. 1878–1893, Aug. 1990.

[2] K. N. Liou, S. C. Ou, Y. Takano, F. P. J. Valero, and T. P. Ackerman, "Remote sounding of the tropical cirrus cloud temperature and optical depth using 6.5 and 10.5 μm radiometers during STEP," *J. Appl. Meteorol.*, vol. 29, no. 8, pp. 715–726, Aug. 1990.

[3] S. C. Ou, K. N. Liou, W. M. Gooch, and Y. Takano, "Remote sensing of cirrus cloud parameters using AVHRR 3.7 and 10.9 μm channels," *Appl. Opt.*, vol. 32, no. 12, pp. 2171–2180, Apr. 1993.

[4] K. Meyer, P. Yang, and B.-C. Gao, "Optical thickness of tropical cirrus clouds derived from the MODIS 0.66- and 1.375- μm channels," *IEEE Trans. Geosci. Remote Sens.*, vol. 42, no. 4, pp. 833–841, Apr. 2004.

[5] M. D. King, W. P. Menzel, P. S. Grant, J. S. Myers, G. T. Arnold, S. E. Platnick, L. E. Gumley, S. C. Tsay, C. C. Moeller, M. Fitzgerald, K. S. Brown, and F. G. Osterwisch, "Airborne scanning spectrometer for remote sensing of cloud, aerosol, water vapor and surface properties," *J. Atmos. Ocean. Technol.*, vol. 13, no. 4, pp. 777–794, Apr. 1996.

[6] MODIS Algorithm Theoretical Basis Document, No. ATBD-MOD-05 M. D. King, S.-C. Tsay, S. E. Platnick, M. Wang, and K. N. Liou, Cloud Retrieval Algorithms for MODIS: Optical Thickness, Effective Particle Radius, and Thermodynamic Phase1996, No. ATBD-MOD-05.

[7] S. Platnick, M. King, S. Ackerman, W. Menzel, B. Baum, J. Riedi, and R. Frey, "The MODIS cloud products—Algorithms and examples from Terra," *IEEE Trans. Geosci. Remote Sens.*, vol. 41, no. 2, pp. 459–473, Feb. 2003.

[8] A. K. Heidinger and M. J. Pavolonis, "Gazing at cirrus clouds for 25 years through a split window. Part I: Methodology," *J. Appl. Meteorol. Climatol.*, vol. 48, no. 6, pp. 1100–1116, Jun. 2009.

[9] B. A. Baum, P. Yang, A. J. Heymsfield, S. Platnick, M. D. King, Y.-X. Hu, and S. T. Bedka, "Bulk scattering properties for the remote sensing of ice clouds. Part II: Narrowband models," *J. Appl. Meteorol.*, vol. 44, no. 12, pp. 1896–1911, Dec. 2005.

[10] T. F. Lee, C. S. Nelson, P. Dills, L. P. Riishojgaard, A. Jones, L. Li, S. Miller, L. E. Flynn, G. Jedlovec, W. McCarty, C. Hoffman, and G. McWilliams, "NPOESS: Next-generation operational global earth observations," *Bull. Amer. Meteorol. Soc.*, vol. 91, pp. 727–740, 2010.

[11] S. C. Ou, Y. Takano, K. N. Liou, G. J. Higgins, A. George, and R. Slonaker, "Remote sensing of cirrus cloud optical thickness and effective particle size for the National Polar-Orbiting Operational Environmental Satellite System Visible Infrared Imager Radiometer Suite: Sensitivity to instrument noise and uncertainties in environmental parameters," *Appl. Opt.*, vol. 42, no. 36, pp. 7202–7214, Dec. 2003.

[12] S. C. Ou, K. N. Liou, Y. Takano, and R. L. Slonaker, "Remote sensing of cirrus cloud particle size and optical depth using polarimetric sensor measurements," *J. Atmos. Sci.*, vol. 62, no. 12, pp. 4371–4383, Dec. 2005.

[13] S. C. Ou, K. N. Liou, Y. Takano, E. Wong, K. Hutchison, and T. Samec, "Comparison of the University of California at Los Angeles line-by-line equivalent radiative transfer model and the moderate-resolution transmission model for accuracy assessment of the National Polar-Orbiting Operational Environmental Satellite System's Visible–Infrared Imager-Radiometer Suite cloud algorithms," *Appl. Opt.*, vol. 44, no. 29, pp. 6274–6284, Oct. 2005.

[14] K. D. Hutchison, E. Wong, and S. C. Ou, "Cloud base height retrieval during nighttime conditions with MODIS data," *Int. J. Remote Sens.*, vol. 27, no. 14, pp. 2847–2862, Jul. 2006.

[15] E. Wong, K. Hutchison, S. C. Ou, and K. N. Liou, "Cirrus cloud top temperatures retrieved from radiances in the National Polar-Orbiting Operational Environmental Satellite System—Visible Infrared Imager Radiometer Suite 8.55 and 12.0 μm bandpasses," *Appl. Opt.*, vol. 46, no. 8, pp. 1316–1325, Mar. 2007.

[16] H. Wei, P. Yang, J. Li, B. A. Baum, H.-L. Huang, S. Platnick, Y. Hu, and L. Strow, "Retrieval of semitransparent ice cloud optical thickness from Atmospheric Infrared Sounder (AIRS) measurements," *IEEE Trans. Geosci. Remote Sens.*, vol. 42, no. 10, pp. 2254–2267, Oct. 2004.

[17] J. Li, H.-L. Huang, C.-Y. Liu, P. Yang, T. J. Schmidt, H. Wei, E. Weisz, L. Guan, and W. P. Menzel, "Retrieval of cloud Microphysical properties from MODIS and AIRS," *J. Appl. Meteorol.*, vol. 44, no. 10, pp. 1526–1543, Oct. 2005.

[18] L. Clarisse, D. Hurtmans, A. J. Prata, F. Karagulian, C. Clerbaux, M. De Mazière, and P.-F. Coheur, "Retrieving radius, concentration, optical depth, and mass of different types of aerosols from high-resolution infrared nadir spectra," *Appl. Opt.*, vol. 49, no. 19, pp. 3713–3722, Jul. 2010.

[19] Q. Yue, K. N. Liou, S. C. Ou, B. H. Kahn, P. Yang, and G. G. Mace, "Interpretation of AIRS data in thin cirrus atmospheres based on a fast radiative transfer model," *J. Atmos. Sci.*, vol. 64, no. 11, pp. 3827–3842, Nov. 2007.

[20] L. M. McMillin, L. J. Crone, M. D. Goldberg, and T. J. Kleespies, "Atmospheric transmittance of an absorbing gas. 4. OPTRAN: A computationally fast and accurate transmittance model for absorbing gases with variable mixing ratios at variable viewing angles," *Appl. Opt.*, vol. 34, no. 27, pp. 6269–6274, Sep. 1995.

[21] S. Chung, S. A. Ackerman, P. F. van Delst, and W. P. Menzel, "Model calculations and interferometer measurements of ice-cloud characteristics," *J. Appl. Meteorol.*, vol. 39, no. 5, pp. 634–644, May 2000.

[22] H. L. Huang, P. Yang, H. L. Wei, B. A. Baum, Y. X. Hu, P. Antonelli, and S. A. Ackerman, "Inference of ice cloud properties from high spectral resolution infrared observations," *IEEE Trans. Geosci. Remote. Sens.*, vol. 42, no. 4, pp. 842–853, Apr. 2004.

[23] Q. Yue and K. N. Liou, "Cirrus cloud optical and microphysical properties determined from AIRS infrared spectra," *Geophys. Res. Lett.*, vol. 36, p. L05810, Mar. 2009.

[24] K. N. Liou, Q. Fu, and T. P. Ackerman, "A simple formulation of the delta-four-stream approximation for radiative transfer parameterizations," *J. Atmos. Sci.*, vol. 45, no. 13, pp. 1940–1948, Jul. 1988.

[25] Q. Fu and K. N. Liou, "Parameterization of the radiative properties of cirrus clouds," *J. Atmos. Sci.*, vol. 50, no. 13, pp. 2008–2025, Jul. 1993.

[26] S. C. Ou, K. N. Liou, Y. Takano, N. X. Rao, Q. Fu, A. J. Heymsfield, L. M. Miloshevich, B. Baum, and S. A. Kinne, "Remote sounding of cirrus cloud optical depths and ice crystal sizes from AVHRR data: Verification using FIRE II IFO measurements," *J. Atmos. Sci.*, vol. 52, no. 23, pp. 4143–4158, Dec. 1995.

[27] S. C. Ou, K. N. Liou, and T. Caudill, "Remote sounding of multilayer cirrus cloud systems using AVHRR data collected during FIRE-II-IFO," *J. Appl. Meteorol.*, vol. 37, no. 3, pp. 241–254, Mar. 1998.

[28] S. C. Ou, K. N. Liou, P. Yang, P. Rolland, T. Caudill, J. Lisowski, and B. Morrison, "Airborne retrieval of cirrus cloud optical and microphysical properties using ARES 5.1–5.3 and 3.7 μm channel data," *J. Geophys. Res.*, vol. 103, no. D18, pp. 23 231–23 242, Sep. 1998.

[29] S. C. Ou, K. N. Liou, M. D. King, and S.-C. Tsay, "Remote sensing of cirrus cloud parameters based on a 0.63–3.7 μm radiance correlation technique applied to AVHRR data," *Geophys. Res. Lett.*, vol. 26, no. 16, pp. 2437–2440, 1999.

[30] K. N. Liou, S. C. Ou, Y. Takano, J. Roskovensky, G. Mace, K. Sassen, and M. Poellot, "Remote sensing of three-dimensional inhomogeneous cirrus clouds using satellite and mm-wave cloud radar data," *Geophys. Res. Lett.*, vol. 29, no. 9, pp. 74-1–74-4, May 2002.

[31] K. N. Liou, S. C. Ou, Y. Takano, and J. Cetola, "Remote sensing of three-dimensional cirrus clouds from satellites: Application to continuous-wave laser atmospheric transmission and backscattering," *Appl. Opt.*, vol. 45, no. 26, pp. 6849–6859, Sep. 2006.

[32] L. Strow, S. Hannon, S. De Souza-Machado, and H. Motteler, "An overview of the AIRS radiative transfer model," *IEEE Trans. Geosci. Remote Sens.*, vol. 41, no. 2, pp. 303–313, Feb. 2003.

[33] L. Strow, S. Hannon, M. Weiler, K. Overoye, S. Gaiser, and H. Aumann, "Pre-launch spectral calibration of the Atmospheric Infrared Sounder (AIRS)," *IEEE Trans. Geosci. Remote Sens.*, vol. 41, no. 2, pp. 274–286, Feb. 2003.

[34] K. N. Liou, S. C. Ou, Y. Takano, and Q. Liu, "A polarized delta-four-stream approximation for infrared and microwave radiative transfer, Part 1," *J. Atmos. Sci.*, vol. 62, no. 7, pp. 2542–2554, Jul. 2005.

[35] B. A. Baum, P. Yang, S. Nasiri, A. K. Heidinger, A. Heymsfield, and J. Li, "Bulk scattering properties for the remote sensing of ice clouds. Part III: High-resolution spectral models from 100 to 3250 cm^{-1}," *J. Appl. Meteorol. Climatol.*, vol. 46, no. 4, pp. 423–434, Apr. 2007.

[36] J. Niu, P. Yang, H.-L. Huang, J. E. Davies, J. Li, B. A. Baum, and Y. X. Hu, "A fast infrared radiative transfer model for overlapping clouds," *J. Quant. Spec. Radiat. Transf.*, vol. 103, no. 3, pp. 447–459, Feb. 2007.

[37] Z. Zhang, P. Yang, G. Kattawar, H.-L. Huang, T. Greenwald, J. Li, B. A. Baum, D. K. Zhou, and Y. Hu, "A fast infrared radiative transfer model based on the adding–doubling method for hyperspectral applications," *J. Quant. Spec. Radiat. Transf.*, vol. 105, no. 2, pp. 243–263, Jun. 2007.

[38] J. Susskind, C. D. Barnet, and J. M. Blaisdell, "Retrieval of atmospheric and surface parameters from AIRS/AMSU/HSB data in the presence of clouds," *IEEE Trans. Geosci. Rem. Sens.*, vol. 41, no. 2, pp. 390–409, Feb. 2003.

[39] M.-D. Chou and L. Kouvaris, "Monochromatic calculations of atmospheric radiative transfer due to molecular line absorption," *J. Geophys. Res.*, vol. 91, no. D3, pp. 4047–4055, 1986.

[40] F. Parol, J.-C. Buriez, G. Brogniez, and Y. Fouquart, "Information content of AVHRR channels 4 and 5 with respect to the effective radius of cirrus cloud particles," *J. Appl. Meteorol.*, vol. 30, no. 7, pp. 973–984, Jul. 1991.

[41] K. N. Liou, Y. Gu, Y. Que, and G. MacFarquhar, "On the correlation between ice water content and ice crystal size and its application to radiative transfer and general circulation models," *Geophys. Res. Lett.*, vol. 35, p. L13805, Jul. 2008. doi:10.1029/2008GL033918.

[42] P. Yang, K. N. Liou, K. Wyser, and D. Mtichell, "Parameterization of the scattering and absorption properties of individual ice crystals," *J. Geophys. Res.*, vol. 105, no. D4, pp. 4699–4718, Feb. 2000.

[43] C. Christiansen, "Untersuchungen über die optischen Eigenschaften von fein verteilten Körpern," *Ann. Phys. Chem.*, vol. 23, pp. 298–306, 1884.

[44] C. Christiansen, "Untersuchungen über die optischen Eigenschaften von fein verteilten Körpern," *Ann. Phys. Chem.*, vol. 24, pp. 439–446, 1885.

[45] K. N. Liou, *An Introduction to Atmospheric Radiation*, 2nd ed. San Diego, CA: Academic, 2002, 583 pp..

[46] B. H. Kahn, C. K. Liang, A. Eldering, A. Gettelman, Q. Yue, and K. N. Liou, "Tropical thin cirrus and relative humidity observed by the Atmospheric Infrared Sounder," *Atmos. Chem. Phys.*, vol. 8, no. 6, pp. 1501–1518, Mar. 2008.

[47] B. H. Kahn, A. Eldering, A. J. Braverman, E. J. Fetzer, J. H. Jiang, E. Fishbein, and D. L. Wu, "Toward the characterization of upper tropospheric clouds using Atmospheric Infrared Sounder and Microwave

Limb Sounder observations," *J. Geophys. Res.*, vol. 112, p. D05202, Mar. 2007.

[48] B. H. Kahn, E. Fishbein, S. L. Nasiri, A. Eldering, E. J. Fetzer, M. J. Garay, and S.-Y. Lee, "The radiative consistency of Atmospheric Infrared Sounder and Moderate Resolution Imaging Spectroradiometer cloud retrievals," *J. Geophys. Res.*, vol. 112, p. D09201, May 2007.

[49] B. H. Kahn, M. T. Chahine, G. L. Stephens, G. G. Mace, R. T. Marchand, Z. Wang, C. D. Barnet, A. Eldering, R. E. Holz, R. E. Kuehn, and D. G. Vane (2008, Mar.). Cloud type comparisons of AIRS, CloudSat, and CALIPSO cloud height and amount. *Atmos. Chem. Phys.* [Online]. *8(5)*, pp. 1231–1248. Available: http://www.atmos-chem-phys.net/8/1231/2008/

[50] E. Weisz, J. Li, W. P. Menzel, A. K. Heidinger, B. H. Kahn, and C.-Y. Liu, "Comparison of AIRS, MODIS, CloudSat and CALIPSO cloud to height retrievals," *Geophys. Res. Lett.*, vol. 34, p. L17811, Sep. 2007.

[51] D. L. Wu, S. A. Ackerman, R. Davies, D. J. Diner, M. J. Garay, B. H. Kahn, B. C. Maddux, C. M. Moroney, G. L. Stephens, J. P. Veefkind, and M. A. Vaughan, "Vertical distributions and relationships of cloud occurrence frequency as observed by MISR, AIRS, MODIS, OMI, CALIPSO, and CloudSat," *Geophys. Res. Lett.*, vol. 36, p. L09821, May 2009.

[52] M. G. Divakarla, C. D. Barnet, M. D. Goldberg, L. M. McMillin, E. Maddy, W. Wolf, L. Zhou, and X. Liu, "Validation of Atmospheric Infrared Sounder temperature and water vapor retrievals with matched radiosonde measurements and forecasts," *J. Geophys. Res.*, vol. 111, p. D09S15, Apr. 2006. doi:10.1029/2005JD006116.

[53] D. C. Tobin, H. E. Revercomb, R. O. Knuteson, B. M. Lesht, L. L. Strow, S. E. Hannon, W. F. Feltz, L. A. Moy, E. J. Fetzer, and T. S. Cress, "Atmospheric radiation measurement site atmospheric state best estimates for Atmospheric Infrared Sounder temperature and water vapor retrieval validation," *J. Geophys. Res.*, vol. 111, p. D09S14, Mar. 2006.

[54] S. Nasiri and B. H. Kahn, "Limitations of bispectral infrared cloud phase determination and potential for improvement," *J. Appl. Meteorol. Climatol.*, vol. 47, no. 11, pp. 2895–2910, Nov. 2008.

[55] H. Jin, S. L. Nasiri, and B. H. Kahn, "Initial assessment of AIRS cloud phase determination," presented at the 13th Conf. Cloud Physics Radiation, Amer. Meteorological Soc., Portland, OR, Jun. 28–Jul. 1, 2010, Paper JP1.20.

[56] J. Susskind, C. Barnet, J. Blaisdell, L. Iredell, F. Keita, L. Kouvaris, G. Molnar, and M. Chahine, "Accuracy of geophysical parameters derived from Atmospheric Infrared Sounder/Advanced Microwave Sounding Unit as a function of fractional cloud cover," *J. Geophys. Res.*, vol. 111, p. D09S17, May 2006.

[57] M. M. Schreier, B. H. Kahn, A. Eldering, D. A. Elliott, E. Fishbein, F. W. Irion, and T. S. Pagano, "Radiance comparisons of MODIS and AIRS using spatial response information," *J. Atmos. Ocean. Technol.*, vol. 27, no. 8, pp. 1331–1342, Aug. 2010.

[58] R. E. Holz, A. Heidinger, D. D. Turner, S. Ackerman, R. Kuehn, M. Vaughan, and S. Platnick, "A characterization of cirrus OD retrievals from active and passive A—Train measurements," presented at the Hyperspectral Imaging Sensing Environment (HISE) Topical Conf., Vancouver, BC, Canada, Apr. 26–30, 2009.

[59] Q. Yang, Q. Fu, and Y. Hu, "Radiative impacts of clouds in the tropical tropopause layer," *J. Geophys. Res.*, vol. 115, p. D00H12, Feb. 2010.

[60] P. Minnis, S. Sun-Mack, Y. Chen, M. M. Khaiyer, Y. Yi, J. K. Ayers, R. R. Brown, X. Dong, S. C. Gibson, P. W. Heck, B. Lin, M. L. Nordeen, L. Nguyen, R. Palikonda, W. L. Smith, Jr., D. A. Spangenberg, Q. Z. Trepte, and B. Xi, "CERES Edition-2 cloud property retrievals using TRMM VIRS and Terra and Aqua MODIS data, Part II: Examples of average results and comparisons with other data," *IEEE Trans. Geosci. Remote Sens.*, vol. 49, no. 11, pp. 4401–4430, Nov. 2011.

[61] S. Kato, F. G. Rose, and T. P. Charlock, "Computation of domain averaged irradiance using satellite-derived cloud properties," *J. Atmos. Ocean. Technol.*, vol. 22, no. 2, pp. 146–164, Feb. 2005.

[62] X. Wang, K. N. Liou, S. S. C. Ou, G. G. Mace, and M. Deng, "Remote sensing of cirrus cloud vertical size profile using MODIS data," *J. Geophys. Res.*, vol. 114, p. D09205, May 2009.

[63] J. M. Comstock, T. P. Ackerman, and G. G. Mace, "Ground-based lidar and radar remote sensing of tropical cirrus clouds at Nauru Island: Cloud statistics and radiative impacts," *J. Geophys. Res.*, vol. 107, p. 4714, Dec. 2002.

[64] T. S. L'Ecuyer, P. Gabriel, K. Leesman, S. J. Cooper, and G. L. Stephens, "Objective assessment of the information content of visible and infrared radiance measurements for cloud microphysical property retrievals over the global oceans. Part I: Liquid clouds," *J. Appl. Meteorol. Climatol.*, vol. 45, no. 1, pp. 20–41, Jan. 2006.

Steve S. C. Ou received the B.S. degree from National Taiwan University, Taipei, Taiwan, in 1972 and the Ph.D. degree from the University of Utah, Salt Lake City, in 1978.

He has been a Postdoctoral Researcher (1979–1980), a Research Assistant Professor (1981–1989), a Research Associate Professor (1989–1997), and a Research Full Professor (1997) with the University of Utah. From 1997 to present, he has been a Research Scientist with the University of California, Los Angeles. He has published more than 60 refereed research papers. For the past two decades, his major effort has been on the development of satellite remote sensing algorithms for cirrus clouds, including the currently operational set of programs for retrieving cirrus cloud height and optical properties that have been implemented in the recently launched National Polar-Orbiting Operational Environmental Satellite System Preparatory Platform System. His research interests span from atmospheric radiative transfer and climate theories and modeling to remote sensing of clouds, dust aerosols, and atmospheric parameters.

Brian Kahn received the B.S. degree in meteorology from San Jose State University, San Jose, CA, in 1995 and the M.S. and Ph.D. degrees in atmospheric sciences from the University of California, Los Angeles, in 2001 and 2004, respectively.

He has worked in collaboration with the NASA Jet Propulsion Laboratory (JPL), Pasadena, CA, as a NASA Postdoctoral fellow from 2005–2008, an Assistant Researcher in the Joint Institute for Regional Earth System Science and Engineering in 2008, and as a staff Research Scientist at JPL since 2009. His research interests focus on the remote sensing of clouds, temperature, and water vapor and their synthesis with multiple satellite instrument platforms to understand cloud-related processes.

Kuo-Nan Liou received the B.S. degree from the National Taiwan University, Taipei, Taiwan, and the Ph.D. degree from New York University, New York.

He is currently a Distinguished Professor of Atmospheric Sciences and Director of the Joint Institute for Regional Earth System Science and Engineering, University of California, Los Angeles. He has authored and coauthored more than 220 peer reviewed papers, invited book chapters, and review articles. He is best known for his two monographs, "An Introduction to Atmospheric Radiation (1980; 2002, 2nd Ed.)" and "Radiation and Cloud Processes in the Atmosphere: Theory, Observation and Modeling (1992)." He was elected to the National Academy of Engineering of the United States in 1999 and served as a past Chair of its Special Fields and Interdisciplinary Engineering Section (2008–2010). He was elected to the Academia Sinica (Chinese Academy of Sciences, Taiwan) in 2004. His current research interests and activities span from regional climate modeling and validation using satellite data to direct and indirect effects of black carbon and dust aerosols on cloud radiative forcing and snow-albedo feedback, radiative transfer in mountains and surface energy balance in climate models, and laboratory light scattering and spectroscopy involving ice particles and absorbing aerosols.

Dr. Liou is a Fellow of the American Association of the Advancement of Science, Optical Society of America, American Geophysical Union, and American Meteorological Society (AMS). He was the recipient of the AMS Jule Charney Award in 1998, shared the 2007 Nobel Peace Prize Certificate bestowed on the Intergovernmental Panel on Climate Change, received the 2010 Committee on Space Research Biennial William Nordberg Medal, and was recently awarded the 2012 International Radiation Commission's Quadrennial Gold Medal.

Yoshihide Takano was born in Tokyo, Japan, in 1953. He received the B.S. degree from Hokkaido University, Sapporo, Japan, in 1975, the M.S. and Ph.D. degrees from Tohoku University, Sendai, Japan, in 1977 and 1982, respectively, and the Ph.D. degree from The University of Utah, Salt Lake City, in 1987.

He was a Postdoctoral Researcher with the University of Alaska Fairbanks, Fairbanks, during 1983–1984. He was an Assistant Research Professor and an Associate Research Professor with The University of Utah from 1990 to 1997. He is currently a Project Scientist with the University of California, Los Angeles.

Mathias M. Schreier received the Diploma degree in meteorology from the University of Munich, Munchen, Germany, in 2003 and the Ph.D. degree from the University of Bremen, Bremen, Germany, in 2007.

In 2009, he joined the Joint Institute for Regional Earth System Science and Engineering at the University of California, Los Angeles, as a Postdoctoral Researcher and has been working there as an Assistant Researcher since 2010, located at the Jet Propulsion Laboratory, Pasadena, CA. His research interests are remote sensing of clouds and atmosphere from different satellite instruments and their possible synergistic use for a better understanding of atmosphere and climate.

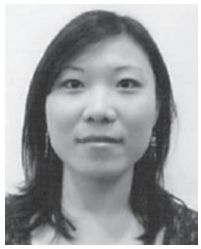

Qing Yue received the B.S. degree in atmospheric physics from Beijing University, Beijing, China, in 2003 and the Ph.D. degree in atmospheric sciences from the University of California, Los Angeles, in 2009.

In the summer of 2009, she joined the Atmospheric Infrared Sounder group at the Jet Propulsion Laboratory, Pasadena, CA, as a Postdoctoral Researcher and worked with Dr. Eric Fetzer. Her research interests are cloud radiative transfer and remote sensing, interaction of cloud, radiation, and water vapor as observed by multiple satellites, and planetary boundary layer clouds.